

# INVESTIGATIONS ON VOLUMETRIC LAYERED TRANSMISSION LINE METAMATERIALS FOR ANTENNA APPLICATIONS

F. Bongard\*, J.R. Mosig\*, M. Van der Vorst<sup>†</sup>

\*Laboratoire d'Electromagnétisme et d'Acoustique (LEMA), Ecole Polytechnique Fédérale de Lausanne (EPFL), Bâtiment ELB, Station 11, CH-1015 Lausanne, Switzerland, E-mail: frederic.bongard@epfl.ch, fax: +41.21.693.26.73

<sup>†</sup>Antenna and Submillimetre Wave Section, European Space Agency (ESA-ESTEC), Keplerlaan 1 PO. Box 299, 2200 AG Noordwijk, The Netherlands, E-mail: maarten.van.der.vorst@esa.int

**Keywords:** Metamaterials, negative refractive index, left-handed medium, CRLH TL, antennas.

## Abstract

This paper presents the investigations on a volumetric negative refractive index metamaterial (MTM) based on the transmission line (TL) approach to be used as a substrate for patch antennas. A prototype of such a structure, obtained by stacking several 1D planar TL based MTM, has been designed and built. Possibilities of using this kind of MTM substrate for the implementation of multi-frequency patch antennas are discussed.

## 1 Introduction

Metamaterials (MTM) are artificial composite materials specifically engineered to produce a desired electromagnetic behaviour. Most of MTM exhibiting a negative refractive index (or left-handed media, LHM) can be found in two rather different classes. The first class concerns MTM made of metallic inclusions in a host dielectric, such as a combination of split-ring resonators (SRR) and thin wires [1]. These structures often exhibit limited bandwidth due to their resonant nature. The second class concerns MTM based on the transmission line (TL) approach. They consist of a host TL periodically loaded with series capacitances and shunt inductances [2, 3]. As these structures do not rely on resonances, a wide-band left-handed behaviour can be achieved. It can be observed that the first class of MTM can result in 3D volumetric structures that can be considered as material filling, whereas the MTM of the second class are essentially used as 1D or 2D guiding or radiating structures, but their ability to be really considered as a medium, that can be coupled from free-space for instance, is not clearly established.

The goal of this work is to examine antenna applications of a new class of volumetric MTM based on the TL approach. This type of structures has been first proposed by Iyer and Eleftheriades in [4], where they suggest that volumetric TL based MTM can be obtained by layering several plates, each one containing a planar 1D or 2D TL based MTM, also called

composite right/left-handed (CRLH) TL [2]. The idea is thus to take benefit of the non resonant nature of TL based MTM for the realization of wideband volumetric MTM that can be considered as material filling and used, for instance, as printed antenna substrate.

The unique features of negative refractive index MTM (or left-handed media), or more generally MTM with both left-handed (LH) and right-handed (RH) bands, have recently produced interesting antenna concepts. For instance, miniaturized resonant antennas can be obtained by making use of the large negative phase constant ( $\beta$ ) that can be achieved at low frequency. This leads to a small guided wavelength  $\lambda_g$  which allows obtaining a  $\lambda_g/2$  field distribution over a physically small distance [5-7]. In addition, Those structures also allows obtaining low values of  $|\beta|$  (positive or negative), hence large values of  $\lambda_g$ , which can be used for the design of enlarged half-wavelength resonant antennas with enhanced gain due to larger radiation aperture [8]. Possibilities of reducing the size of resonant antennas using pairs of complementary materials by phase compensation [9] have also been discussed [10, 11]. MTM with negative refractive index, or with both LH and RH bands, have also been used for the realization of leaky-wave antennas operating in the fundamental mode [2, 12, 13], with the unique feature of broadside radiation capability. Finally, using several resonant operating points in the dispersion diagram allows implementing dual-mode [14] or dual-frequency [15] MTM based antennas by combining several of the principles described above. It can be noted that most of these antenna concepts use MTM based on the TL approach, but there is no fundamental limitation for their implementation with volumetric inclusion-based MTM.

The paper is organized as follows. First, CRLH TL implemented in coplanar stripline (CPS) have been investigated by full wave simulations and equivalent circuit models (section 2). Then, the effect of stacking these structures one on top the other has been analysed by means of dispersion diagrams obtained for various configurations (section 3). Finally, potential applications of such volumetric TL based MTM as substrates for microstrip patch antennas are discussed (section 4).

## 2 CRLH TL implemented in CPS

### 2.1 Description

The host TL which is chosen for implementing the desired stacked structures is the coplanar stripline (CPS), as suggested in [4]. Many examples of TL based MTM, or CRLH TL, implemented in microstrip or CPW are available in the literature [2, 3], whereas CPS implementations are less common. Some examples can however be found in [16, 17]. Figure 1 shows an example of 2-cells CRLH TL implemented in CPS, as well as the corresponding equivalent circuit for the unit cell. In this particular implementation, the series capacitors are implemented as MIM capacitors simply by using the other face of the substrate, whereas meander lines are used for the shunt inductors. It can be observed that because of the chosen topology of capacitors, one cell over two is printed on the other side of the substrate (in dark in the figure), resulting in a  $2d$ -periodic structure. A true  $d$ -periodic structure can be obtained by using vertical connections just after each MIM capacitor to come back to the upper side of the substrate. However, these two versions being almost equivalent in terms of  $S$  parameters, it is believed that the structure of Figure 1 can be considered as  $d$ -periodic.

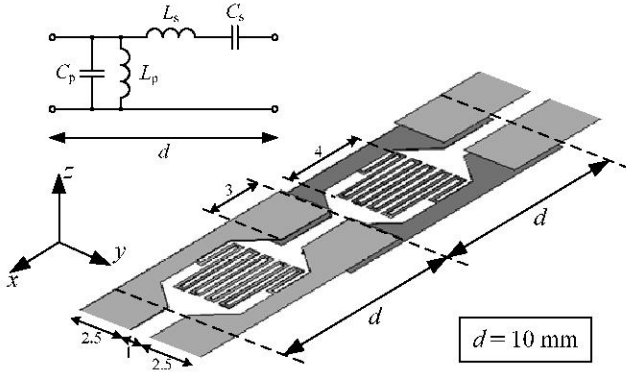


Figure 1: 1D CRLH TL implemented in CPS, with equivalent circuit for the unit cell. All the dimensions are in mm. The width of the meander lines is  $150 \mu\text{m}$ . The substrate, which is not shown for clarity, is: Rogers RT/Duroid 5870 ( $\epsilon_r = 2.33$ ,  $\tan\delta = 0.0012$ , thickness  $h = 0.254 \text{ mm}$ ). The characteristic impedance of the host TL is  $Z_0 = 166 \Omega$ . Extracted values for the circuit elements are  $C_s = 386 \text{ fF}$ ,  $L_p = 12.1 \text{ nH}$ ,  $C_p = 203 \text{ fF}$  and  $L_s = 9.34 \text{ nH}$ .

### 2.2 Performances

The equivalent (or Bloch) propagation constant and characteristic impedances of a periodic structure can be deduced from the transfer (or  $ABCD$ ) matrix of a single unit cell using the Floquet Theorem [2, 3]. Figure 2 shows the equivalent propagation constant ( $\gamma_{\text{equ}}$ ) (or dispersion diagram) for the structure shown in Figure 1.

A good agreement is observed between full wave and equivalent circuit results (the curves are almost superimposed). This structure exhibits a left-handed behaviour over a  $1.58 \text{ GHz}$  bandwidth between  $f_{\text{CL}}$  and  $f_s$ .

Moreover, it is not balanced [2] since a stop band exists between  $f_s$  and  $f_p$ . Making this structure balanced could be achieved by tuning the dimensions of the layout elements, if required for a particular application.

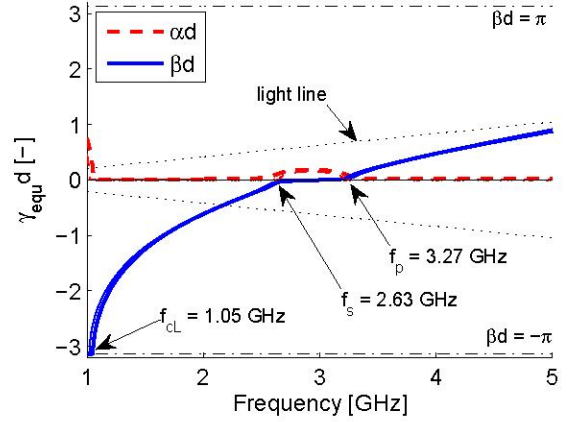


Figure 2: Equivalent propagation constant for the CPS CRLH TL shown in Figure 1, extracted from the  $ABCD$  matrix of a single unit cell. Thick line: full wave simulation (HFSS), thin line: equivalent circuit.

The limit frequencies  $f_s$  and  $f_p$  can be calculated from the equivalent circuit as follows:

$$f_s = \frac{1}{2\pi\sqrt{L_s C_s}} \quad \text{and} \quad f_p = \frac{1}{2\pi\sqrt{L_p C_p}} \quad (1)$$

The corresponding expression for  $f_{\text{CL}}$  can be found in [2]. Using these expressions and the extracted elements values, we find  $f_s = 2.65 \text{ GHz}$ ,  $f_p = 3.21 \text{ GHz}$  and  $f_{\text{CL}} = 1.02 \text{ GHz}$ , which is close to the values deduced from the full wave results (see Figure 2). It is also worth mentioning that at the upper limit of the LH band ( $f_s = 2.63 \text{ GHz}$ ), the unit cell is about 10 times smaller than the guided wavelength in the host TL, which is favourable for considering this kind of periodic structures as effectively homogeneous [2].

Potential applications of such CPS CRLH TL are leaky wave antennas using the principle described in [2, 12, 13], or series-fed dipole arrays [16]. For the present work we are more interested in volumetric MTM that can be derived from these structures, as described in section 3.

## 3 Volumetric layered TL based MTM

### 3.1 Principle

The concept of volumetric layered TL based MTM has been first introduced in [4]. These structures actually consist of a stacking of planar CRLH TL implemented in CPS, that should behave as an equivalent medium exhibiting a negative refractive index for some particular propagation directions and polarizations. The idea is to take benefit of the non resonant nature of TL based MTM for the realization of wideband volumetric negative refractive index MTM that can be considered as material filling. In [4], a 3D MTM obtained by stacking 2D isotropic TL based MTM has been presented.



We consider here a variant of this class of structures, namely a stacking of 1D CPS CRLH TL similar to that shown in Figure 1, as suggested in Figure 3. We do not consider here the possibility of replicating the structure in the lateral direction  $y$ , since we are more interested in obtaining a thin MTM slab to be used as printed antenna substrate. The obtained volumetric structure, although not isotropic, is expected to exhibit a negative refractive index (or left-handed behaviour) for propagation along  $x$ .

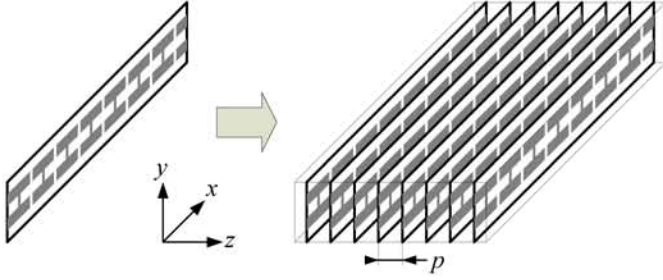


Figure 3: Stacking 1D CPS CRLH TL to create a volumetric MTM slab, following the idea introduced in [4].

### 3.2 Effect of stacking

First, we investigate the effect of stacking on the properties of the CRLH TL. For that purpose, we consider an infinite periodic structure (with periodicity  $p$ ) along the transverse direction  $z$ . For propagation along  $x$ , the fields around each CRLH TL are the same, as suggested in Figure 4.

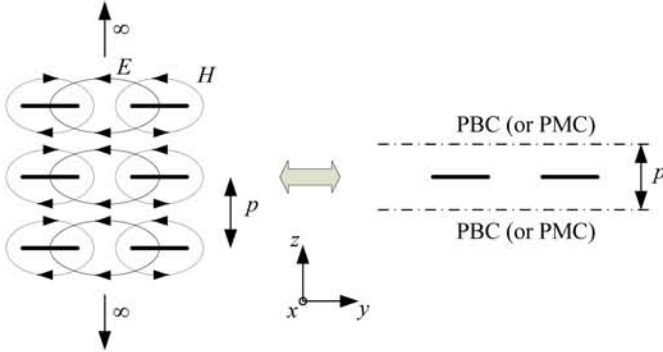


Figure 4: Stacking of CPS (transverse view), and equivalent structure if the fields are the same in each vertical unit cell. Perfect magnetic conductors (PMC) are equivalent to periodic boundary conditions (PBC) if the unit cell is symmetric along  $z$ .

For numerical analyses, a single CPS CRLH TL is considered, making use of PMC to approximate the transverse periodicity (PBC are not compatible with wave ports in HFSS). A parametric study on the dependence of some parameters of the CRLH TL with the transverse periodicity  $p$  has been carried out. The main results are summarized below:

- The characteristic impedance of the host TL ( $Z_c$ ) increases when  $p$  decreases.
- $L_p$  and  $C_p$  decreases with  $p$ .
- $L_s$  increases when  $p$  decreases.
- $C_s$  slightly increases when  $p$  decreases.

As a result,  $f_s$  decreases and  $f_p$  increases when  $p$  decreases, which means that satisfying the balanced condition [2]

$$f_s = f_p, \quad \text{or} \quad L_s C_s = L_p C_p \quad (2)$$

becomes more difficult for lower values of  $p$ , for comparable dispersion diagrams, mainly because obtaining high values of  $L_p$  can be rather challenging. To complete the picture, Figure 5 shows the influence of  $p$  on the dispersion diagram for a stacking of CRLH TL similar to that described in Figure 1 (but with different parameters).

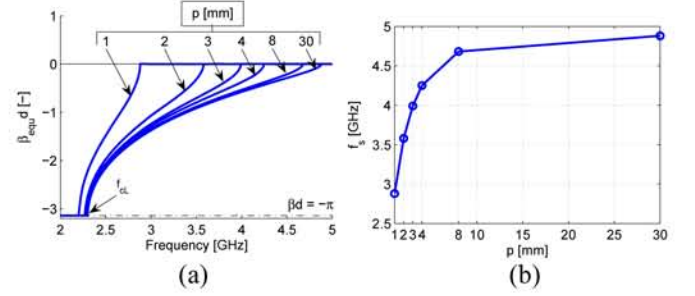


Figure 5: (a) Influence of the transverse periodicity  $p$  on the dispersion diagram of a stacking of CPS CRLH TL similar to that shown in Figure 1 (the RH band is out of the considered frequency range). (b) Evolution of  $f_s$ , the upper limit of the LH band.

It can be observed that the lower limit of the LH band ( $f_{cl}$ ) is almost not affected by the stacking, whereas the upper limit  $f_s$  considerably decreases with  $p$ . Therefore, a trade-off has to be made for the selection of  $p$ . It has to be small enough in order to obtain a bulk structure which has more chances to behave as an equivalent medium, but it should not be too small in order to keep a reasonably large LH band that will be further exploited. A value around  $p = 4$  mm has been chosen for further investigations.

### 3.3 Description of the realized volumetric TL based MTM

Taking into account the considerations of the section 3.2, a 1D CRLH TL to be used for the stacking has been designed. It is shown in Figure 6.

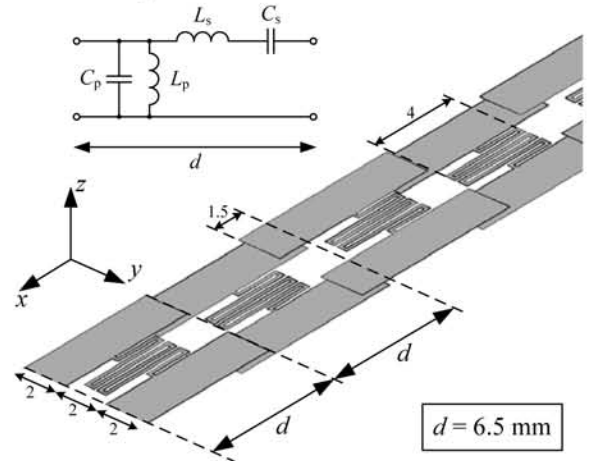


Figure 6: 1D CPS CRLH TL to be used for the stacking (similar to Figure 1).

The volumetric layered TL based MTM is obtained by stacking this planar structure in the  $z$  direction with transverse periodicity  $p = 4.254$  mm. A picture of the realized prototype, which will be called the "meta-slab", can be seen in Figure 7. It consists of 27 plates, each one containing a CRLH TL with 19 unit cells. Layers of foam (Rohacell,  $\epsilon_r = 1.07$ ) of thickness 4 mm have been stuck between the plates. The dispersion diagram for this structure for propagation along  $x$  is show in Figure 8.

This structure exhibits a left-handed behaviour over a 2.13 GHz bandwidth between  $f_{cL}$  and  $f_s$ . At the upper limit of the LH band ( $f_s = 4.21$  GHz), the unit cell is about 10 times smaller than the guided wavelength in the host TL.

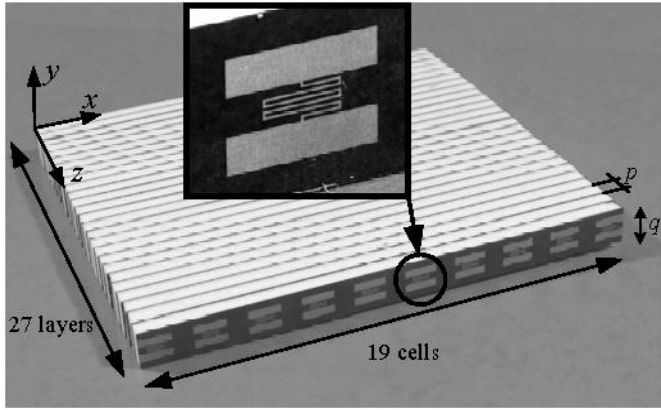


Figure 7: Picture of the realized volumetric layered TL based MTM (or meta-slab). The slab thickness is  $q = 10$  mm. The overall dimensions of the meta-slab are approximately  $111 \times 125 \times 10$  mm.

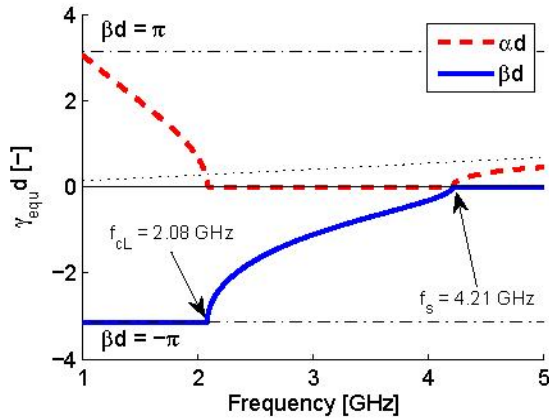


Figure 8: Dispersion diagram for the meta-slab for propagation along  $x$ , obtained by extraction from the  $ABCD$  matrix of a single unit cell (full wave results), as explained in section 2.2.

### 3.4 Meta-slab in microstrip configurations

It is desirable to use the realized meta-slab as a substrate in a microstrip configuration like a patch antenna, for instance. However, the presence of metal plates (ground plane and/or patch) at proximity of the structure strongly affects its

dispersion diagram, as explained thereafter. The two cases that are analyzed are illustrated in Figure 9.

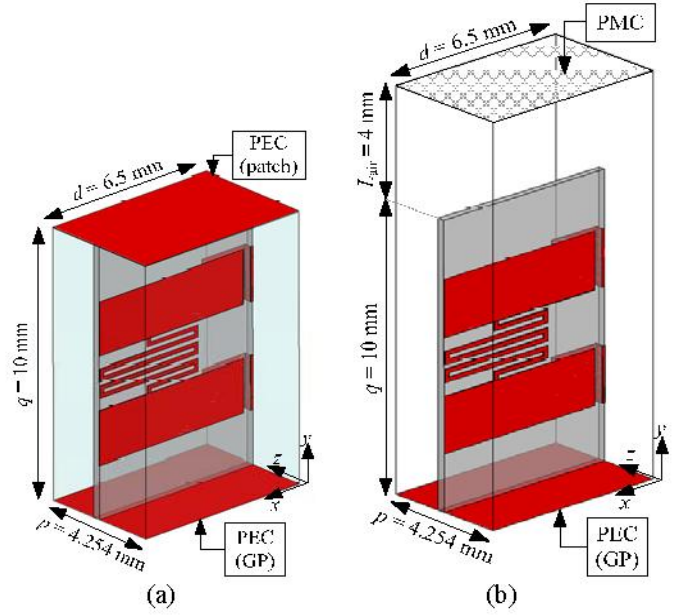


Figure 9: Unit cell of the meta-slab (a) in a parallel plate waveguide (PPWG), (b) above a ground plane (GP), where PMC is applied on the top of the unit cell to close the structure for full wave analysis with HFSS. PBC are applied on the four vertical walls of the unit cell. It can be noted that the MIM series capacitors have been slightly modified to obtain a true  $d$ -periodic structure, as required for eigenmode analyses.

In both cases, the structure is now a periodically loaded multiconductor TL, and therefore several quasi-TEM modes may propagate along it (along the  $x$  direction). As a consequence, a simple extraction of the dispersion diagram from monomode  $ABCD$  matrix is not possible anymore. Two other methods have been used to obtain the dispersion diagram:

- Eigenmode analysis with the eigensolver of HFSS.
- Extraction from multimode  $ABCD$  matrix of the unit cell. This is an extension of the method for "monomode" periodic structures already discussed in section 2.2, for the multimode (or multiconductor) case (this method is not detailed here).

The dispersion diagram for the case shown in Figure 9(a) is shown in Figure 10, whereas Figure 11 shows the comparison between the different configurations.

A good correspondence can be observed between the two methods, with the main difference being the revelation of a complex mode band (both  $\alpha, \beta \neq 0$ ) by the extraction from multimode analysis, which is not obtained by the eigenmode analysis. With the latter method we obtain a stop band. It can be noted that the multimode analysis required about 9 minutes of full wave simulation against 5 hours for the eigenmode analysis.



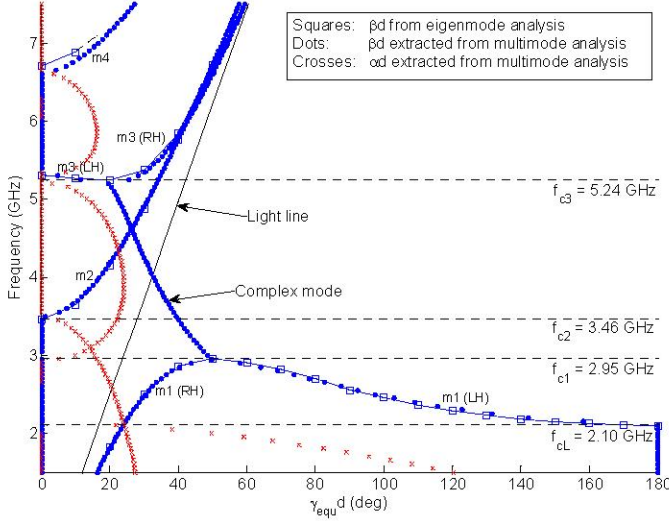


Figure 10: Dispersion diagram for propagation along  $x$  for the structure shown in Figure 9(a), obtained with the two proposed methods.

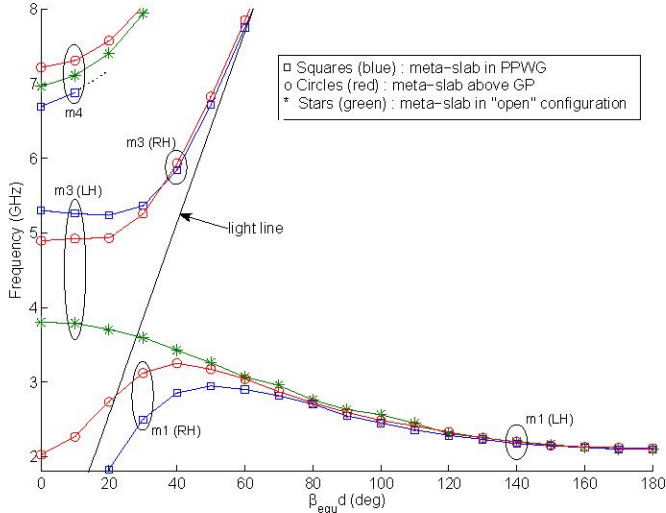


Figure 11: Comparison of dispersion diagrams (obtained by eigenmode analysis) between the two structures shown in Figure 9 and the "open" configuration already studied in section 3.3. Only the modes of interest are shown. The ellipses suggest how the modes should correspond.

In comparison with the "open" configuration studied in section 3.3 (see Figure 11), we observe an additional stop band (or complex mode band according to the multimode analysis) which results from contra-directional coupling between the LH CPS mode and the RH PPWG mode. As a result, the useable LH band is reduced compared to the "open" configuration. In the complex mode band, we have in fact two modes with complex-conjugate propagation constants, a phenomenon associated with mode conversion between the two coupled modes. Moreover, for a given frequency in the LH band, both the "m1 (LH)" and the "m1 (RH)" modes can propagate (or the "m3 (LH)" and "m3 (RH)" modes at higher frequencies). All these phenomena have already been observed and discussed for the shielded mushroom structure [18].

### 3.5 Experimental verification

A simple measurement has been performed for a first evaluation of the qualitative behaviour of the meta-slab in a microstrip configuration. The  $S$  parameters of a microstrip line using the meta-slab as substrate have been measured with a HP8510C network analyser by means of a TRL calibration (Figure 12). The width of the strip is rather large ( $w = 17 \text{ mm} \cong 4p$ ) such that the meta-MS line locally behaves as the meta-slab in a PPWG, which unit cell is shown in Figure 9(a).

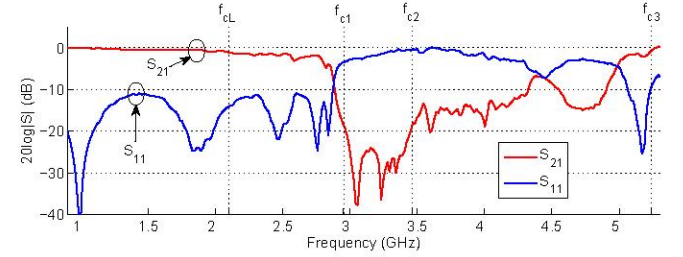


Figure 12: Measured  $S$  parameters of a MS line using the meta-slab as substrate. The strip is parallel to the CRLH TL that form the meta-slab (along  $x$ ).

It can be observed that the stop band predicted in the dispersion diagram of Figure 10 (between  $f_{c1}$  to  $f_{c2}$ ) can be seen on the measured  $S$  parameters. The band from  $f_{c2}$  to  $f_{c3}$  has mainly a stop band behaviour, which may indicate that the mode "m2" is only slightly excited. Between  $f_{cL}$  and  $f_{c1}$ , the structure may support the propagation of both the LH and RH modes. However, it is not evident to evaluate to which extend the LH mode is excited simply by looking at the  $S$  parameters.

## 4 Applications to microstrip antennas

### 4.1 Basic description and motivations

The goal is to investigate potential applications of the designed meta-slab for microstrip (MS) patch antennas where the meta-slab is used as a substrate, as shown in the example of Figure 13. This kind of structures will be called "meta-patches". Among the various potential applications of such negative refractive index MTM slab (see section 1), the one targeted here concerns the exploitation of several resonant operating points in the dispersion diagram for the implementation of multi-frequency MTM based antennas.

### 4.2 Resonant frequencies

Let us consider a rectangular patch of length  $L = Nd$ , where  $N$  is the number of cells covered by the patch in the longitudinal direction ( $x$ ). Then, we make use of the cavity model of patch antennas [19] to derive the possible resonant frequencies. More precisely, we consider that the space below the patch forms a cavity closed all around by PMC. Locally, the meta-patch behaves like the meta-slab in a PPWG shown in Figure 9(a), and which dispersion diagram is shown in Figures 10



and 11. A slice of such an equivalent cavity is shown in Figure 14.

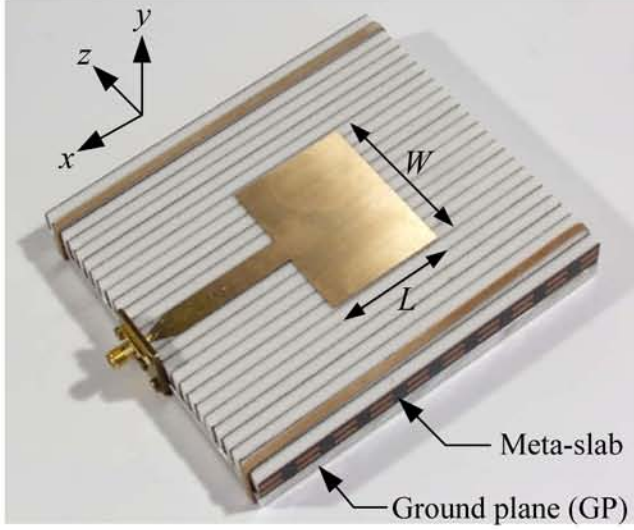


Figure 13: Example of "meta-patch" of size  $L \times W$ , where  $L = Nd = 39$  mm ( $N = 6$  and  $d = 6.5$  mm), and  $W = 50.7$  mm.

The possible resonant frequencies can be deduced from the dispersion diagram using Eq. (3).

$$\beta_{\text{equ}} d = \frac{n\pi}{N}, \quad n \in \mathbb{Z} \quad (3)$$

For odd values of  $n$  (odd modes) the electric fields at the two radiating edges of the patch are out of phase, leading then to constructive interferences at broadside. For even values of  $n$  (even modes) the electric fields at the two radiating edges of the patch are in phase, leading then to destructive interferences at broadside, hence a null of radiation in that direction.

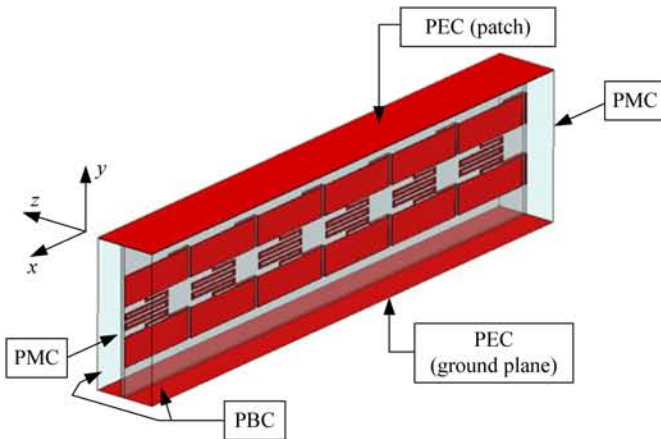


Figure 14: Equivalent cavity for a meta-patch of  $N$  cells ( $N = 6$  in the figure). As we are only interested in modes with fields' variation along  $x$ , a single row of cells is considered and periodic boundary conditions (PBC) are applied in the  $z$  direction to account for the transverse periodicity, which therefore becomes infinite.

Small meta-patches ( $N \leq 4$ ) exhibit resonant frequencies at which the patch is quite small in terms of free-space wavelength (in the range  $0.1 - 0.2 \lambda_0$ ), which could be interesting for miniaturization. This phenomenon has already been exploited with patches made of mushroom-like structures [5-7].

Larger meta-patches are less interesting in terms of miniaturization, but they offer interesting multi-frequency capabilities. More precisely, if we focus on the mixed RH-LH band of the dispersion diagram, that is the band from  $f_{\text{cl}} = 2.10$  GHz to  $f_{\text{cl}} = 2.95$  GHz (see Figure 10), we can obtain several close resonant frequencies corresponding to odd modes (odd values of  $n$ ), in comparison with conventional patches where those frequencies are harmonically related. We consider here an example of a meta-patch of  $N = 6$  cells, whose resonant frequencies ( $f_{\text{res}}$ ) corresponding to the first mixed RH-LH mode are listed in Table 1.

$n$	$\beta_{\text{equ}} d [^\circ]$	$f_{\text{res}} [\text{GHz}]$	
		(a)	(b)
+1	+30	2.50	2.49
-2	-60	2.90	2.91
-3	-90	2.55	2.60
-4	-120	2.28	2.34
-5	-150	2.14	2.19
-6	-180	2.10	-

Table 1: First resonant frequencies ( $f_{\text{res}}$ ) for a meta-patch of  $N = 6$  cells. (a) Extracted from the dispersion diagram. (b) Eigenfrequencies of the cavity shown in Figure 14 calculated with HFSS.

It can be seen that three close odd resonances exist, at 2.14 GHz ( $n = -5$ ), 2.50 GHz ( $n = +1$ ) and 2.55 GHz ( $n = -3$ ). Around those resonant frequencies, the length of the patch is about 0.3 free-space wavelength. It is worth noting that the effect of fringing fields at the edges of the patch (increase of its effective length) have not been considered for the deduction of the resonant frequencies.

The goal is now to investigate whether the resonances highlighted in section 4.2 can be excited with usual feeding techniques used for MS patch antennas [19]. It can be anticipated that the main problem will come from the mixed RH-LH nature of the mode of interest. Indeed, most of the resonant frequencies lie in the LH branch whereas the natural field existing below a patch is more consistent with that of the RH branch. Two feeding techniques are being experimentally tested: microstrip line (as shown in Figure 13) and aperture coupling through the ground plane. A measurement campaign is under way and more results will be presented at the conference.

## 5 Conclusion

A particular realization of a volumetric negative refractive index MTM based on the TL approach has been presented. It consists of a stacking of 1D CRLH TL implemented in CPS. First, it has been observed that stacking these CRLH TL leads

to a reduction of the usable LH band, compared to a single CPS CRLH TL. The designed MTM, which has been called the meta-slab, exhibits a LH behaviour over a 2.13 GHz bandwidth, between 2.08 and 4.21 GHz, with a unit cell about 10 times smaller than the guided wavelength.

Then, the band structure of the meta-slab when used in a microstrip configuration has been investigated. It has been observed that the presence of the ground plane and/or a patch strongly affects the dispersion diagram. One of the main issues is the existence of a dual mode (mixed RH-LH) behaviour at low frequency, in conjunction with a significant reduction of the usable LH band compared to the initial "open" configuration. These phenomena are due to contra-directional coupling between LH and RH modes.

Finally, applications of the meta-slab as substrate for patch antennas have been discussed, with special emphasis on multi-frequency capability. More precisely, we can obtain several close resonant frequencies corresponding to odd modes, in comparison with conventional patches where those frequencies are harmonically related.

Further work concerns the experimental verification of the properties of these meta-patch antennas using various feeding techniques like MS line or slot in the ground plane. The main goal will be to determine to which extend the predicted resonances of the meta-patches can be excited using these feeding techniques.

## Acknowledgements

This work has been supported by the European Space Agency (ESA-ESTEC) under contract 18545/04/NL/LvH and by the Swiss Government under its associated participation to the FP6 - NoE Metamorphose.

## References

- [1] D. R. Smith, W. J. Padilla, D. C. Vier, S. C. Nemat-Nasser, and S. Schultz, "Composite Medium with Simultaneously Negative Permeability and Permittivity," *Physical Review Letters*, vol. 84, pp. 4184-4187, 1 May 2000.
- [2] C. Caloz and T. Itoh, *Electromagnetic Metamaterials: Transmission Line Theory and Microwave Applications*: Wiley-Interscience and IEEE press, 2006.
- [3] G. V. Eleftheriades and K. G. Balmain, *Negative-Refractive Metamaterials: Fundamental Principles and Applications*: Wiley-Interscience and IEEE press, 2005.
- [4] A. K. Iyer and G. V. Eleftheriades, "Volumetric layered transmission-line metamaterial exhibiting a negative refractive index," *Journal of the Optical Society of America B*, vol. 23, pp. 553-570, March 2006.
- [5] M. Schüssler, J. Freese, and R. Jakoby, "Design of Compact Planar Antennas using LH-Transmission Lines," in *IEEE MTT-S Digest*, 2004, pp. 209-212.
- [6] C. J. Lee, K. M. K. H. Leong, and T. Itoh, "Design of Resonant Small Antenna Using Composite Right/Left-Handed Transmission Line," in *IEEE AP-S Int. Symp. and USNC/URSI Meeting*, Washington, DC, 2005.
- [7] C. J. Lee, K. M. K. H. Leong, and T. Itoh, "Composite Right/Left-Handed Transmission Line Based Compact Resonant Antennas for RF Module Integration," *IEEE Transactions on Antennas and Propagation*, vol. 54, pp. 2283-2291, August 2006.
- [8] A. Rennings, S. Otto, C. Caloz, and P. Waldow, "Enlarged Half-Wavelength Resonator Antenna With Enhanced Gain," in *IEEE AP-S Int. Symp. and USNC/URSI Meeting*, Washington, DC, 2005, pp. 683-686.
- [9] N. Engheta, "An Idea for Thin Subwavelength Cavity Resonators Using Metamaterials With Negative Permittivity and Permeability," *IEEE Antennas and Wireless Propagation Letters*, vol. 1, pp. 10-13, 2002.
- [10] S. A. Tretyakov and M. E. Ermutlu, "Modeling of Patch Antennas Partially Loaded With Dispersive Backward-Wave Materials," *IEEE Antennas and Wireless Propagation Letters*, vol. 4, pp. 266-269, 2005.
- [11] A. Alu, F. Bilotti, N. Engheta, and L. Vegni, "Subwavelength, Compact, Resonant Patch Antennas Loaded With Metamaterials," *IEEE Transactions on Antennas and Propagation*, vol. 55, pp. 13-25, January 2007.
- [12] A. Grbic and G. V. Eleftheriades, "Experimental verification of backward-wave radiation from a negative refractive index metamaterial," *Journal of Applied Physics*, vol. 92, pp. 5930-5935, 15 November 2002.
- [13] L. Liu, C. Caloz, and T. Itoh, "Dominant mode leaky-wave antenna with backfire-to-endfire scanning capability," *Electronics Letters*, vol. 38, pp. 1414-1416, 7 November 2002.
- [14] A. Lai, K. M. K. H. Leong, and T. Itoh, "Dual-Mode Compact Microstrip Antenna Based on Fundamental Backward Wave," in *Asia-Pacific Microwave Conference*, 2005.
- [15] S. Otto, A. Rennings, C. Caloz, P. Waldow, and T. Itoh, "Composite Right/Left-Handed Lamda-Resonator Ring Antenna for Dual-Frequency Operation," in *IEEE AP-S Int. Symp. and USNC/URSI Meeting*, Washington, DC, 2005, pp. 684-687.
- [16] M. A. Antoniades and G. V. Eleftheriades, "A Metamaterial Series-Fed Linear Dipole Array with Reduced Beam Squinting," in *APS International Symposium, IEEE*, 2006, pp. 4125-4128.
- [17] R. Goto, H. Deguchi, and M. Tsuji, "Composite Right/Left-Handed Transmission Lines Based on Conductor-Backed Coplanar Strips," *IEICE Trans. Electron.*, vol. E89-C, pp. 1306-1311, September 2006.
- [18] F. Elek and G. V. Eleftheriades, "Dispersion Analysis of the Shielded Sievenpiper Structure Using Multiconductor Transmission-Line Theory," *IEEE Microwave and Wireless Components Letters*, vol. 14, pp. 434-436, September 2004.
- [19] C. A. Balanis, *Antenna Theory, Analysis and Design*: John Wiley & Sons, 1997.